

# Wave modes trapped in rotating nonlinear potentials

Yongyao Li<sup>1,2</sup>, Wei Pang<sup>3</sup>, and Boris A. Malomed<sup>1</sup>

<sup>1</sup>*Department of Physical Electronics, School of Electrical Engineering,  
Faculty of Engineering, Tel Aviv University, Tel Aviv 69978, Israel*

<sup>2</sup>*Department of Applied Physics, South China Agricultural University, Guangzhou 510642, China*

<sup>3</sup>*Department of Experiment Teaching, Guangdong University of Technology, Guangzhou 510006, China.*

We study modes trapped in a rotating ring with the local strength of the nonlinearity modulated as  $\cos(2\theta)$ , where  $\theta$  is the azimuthal angle. This modulation pattern may be of three different types: self-focusing (SF), self-defocusing (SDF), and alternating SF-SDF. The model, based on the nonlinear Schrödinger (NLS) equation with periodic boundary conditions, applies to the light propagation in a twisted pipe waveguide, and to a Bose-Einstein condensate (BEC) loaded into a toroidal trap, under the action of the rotating nonlinear *pseudopotential* induced by means of the Feshbach resonance in an inhomogeneous external field. In the SF, SDF, and alternating regimes, four, three, and five different types of stable trapped modes are identified, respectively: even, odd, second-harmonic (2H), symmetry-breaking, and 2H-breaking ones. The shapes and stability of these modes, together with transitions between them, are investigated in the first rotational Brillouin zone. Ground-state modes are identified in each regime. Boundaries between symmetric and asymmetric modes are also obtained in an analytical form, by of a two-mode approximation.

PACS numbers: 42.65.Tg; 03.75.Lm; 47.20.Ky; 05.45.Yv

## I. INTRODUCTION

Optical and matter waves exhibit a plenty of dynamical scenarios under the action of effective nonlinear potentials (which may sometimes be combined with usual linear potentials) [1]. The dynamics of such systems is governed by the nonlinear Schrödinger equation (NLSE) in optical media, or Gross-Pitaevskii equation (GPE) in the context of Bose-Einstein condensates (BECs). In either case, the nonlinear *pseudopotential* [2] may be induced by a regular [3, 4] or singular [5] spatial modulation of the local nonlinearity. These systems have been studied theoretically in a variety of one- [3, 5] and two-dimensional (1D and 2D) [4] settings, and recently reviewed in Ref. [1]. To the same general class belong models which predict that, in any dimension  $D$ , stable fundamental and vortex solitons can be supported by a purely self-defocusing (SDF) nonlinearity growing towards the periphery ( $r \rightarrow \infty$ ) at any rate faster than  $r^D$  [6].

In optics, such nonlinear potentials may be designed using the mismatch between the nonlinearity of the host material and solid [7] or liquid [8] stuff filling voids of photonic-crystal-fiber waveguides. Another possibility to create the effective nonlinear potential in optics is offered by inhomogeneous distributions of dopants which induce the resonantly enhanced nonlinearity [9]. In particular, it is possible to use the Rhodamine B dopant added to the SU-8 polymer (a commonly used transparent negative photoresist) [10], or  $\text{Pr}^{3+}$  ions doping the  $\text{Y}_2\text{SiO}_5$  host medium [11, 12].

In BEC, the pseudopotential can be created with the help of the Feshbach resonance controlled by nonuniform magnetic [13] or optical [14] fields. In particular, the necessary pattern of the spatial modulation of the scattering length, which determines the local strength of the cubic nonlinearity in the respective GPE, can be induced by appropriately designed magnetic lattices [15].

Another well-known tool for the creation of various dynamical states is provided by rotating potentials, which may trap optical and matter waves. Effects of the rotation have drawn a great deal of attention in the studies of BEC. A well-known results is that rotational stirring of the condensate with repulsive interactions leads to the formation of vortex lattices, see review [16]. Under special conditions (the compensation of the trapping by the centrifugal force), giant vortices can be produced too, which were studied in detail experimentally [17] and theoretically [18]. In a binary immiscible BEC, vortex streets were predicted to form, instead of the vortex lattices [19]. On the other hand, it was predicted that the rotation of self-attractive condensates gives rise to several species of localized modes, such as solitary vortices, mixed-vorticity states (“crescents”), and quasi-solitons [20].

It is natural too to consider the dynamics of matter-wave modes trapped in rotating lattices, which can be created in BEC by broad laser beams transmitted through a revolving mask [21]. Quantum states and vortex lattices have been studied in this setting [22], as well as the depinning of trapped solitons and solitary vortices when the rotation rate exceeds a critical value [23]. The nucleation of vortices in the rotating lattice was demonstrated experimentally [24].

In optics, a setting similar to the rotating lattice can be realized in twisted photonic-crystal fibers [25, 26]. In plain optical fibers, the twist affects the polarization dynamics [27] and couples it to the transmission of temporal

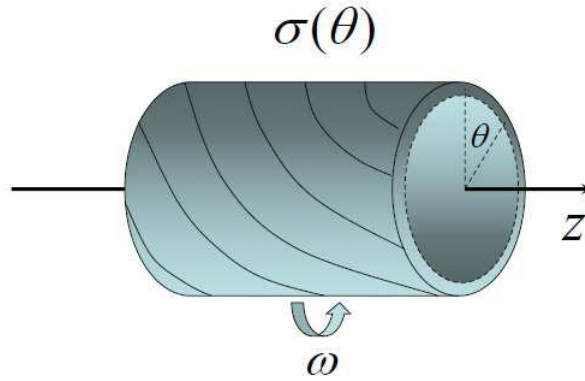


FIG. 1: (Color online) The pipe nonlinear waveguide with the intrinsic nonlinear potential, twisted at rate  $\omega$

solitons [29]. In helical photonic-crystal fibers, modified Bragg reflection and enhancement of the mode conversion and transport have been studied [28], and the transformation of the linear momentum of photons into the orbital angular momentum has been demonstrated recently [26].

The simplest version of the rotating lattice is represented by the revolving quasi-1D double-well potential (DWP). It gives rise to azimuthal Bloch bands [30], and allows one to support solitons and solitary vortices even in the case of the SDF nonlinearity [31]. The generation of a vortex lattice in the rotating DWP was studied too [32]. Further, it is well known that the interplay of the DWP with the SF or SDF nonlinearity provides for the simplest setting for the study of the spontaneous symmetry breaking of even and odd states, respectively, in one dimension [33]. In this connection, a natural problem, which was recently considered in Ref. [34], is a modification of the symmetry-breaking scenarios in a rotating ring carrying the DWP potential, along with the nonlinearity.

While the dynamics of nonlinear waves trapped in rotating linear potentials has been studied in detail, previous works did not tackle modes pulled by rotating *nonlinear* (pseudo-) potentials. This setting, which may be implemented in optics and BEC alike, is the subject of the present work. To analyze the basic features of the respective phenomenology, we here concentrate on the 1D nonlinear potential on a rotating ring, as shown in Fig. 1. In optics, this system is realized as a pipe (hollow) waveguide with an azimuthal modulation of the local nonlinearity,  $\sigma(\theta)$  ( $\theta$  is the angular coordinate), *twisted* with pitch  $2\pi/\omega$ , where  $\omega$  plays the role of the effective rotation speed. In BEC, a similar setting corresponds to a toroidal trap, which is available in the experiment [35], combined with the rotating nonlinear potential, that can be superimposed on top of the trap [36]. This combination realizes a *rotating ring* [37] carrying the nonlinear potential.

It is necessary to define the sign of the nonlinear potential. In this work, we consider three distinct cases, namely, the SF (attractive), SDF (repulsive), and SF-SDF (alternating) nonlinearities, all subject to the harmonic spatial modulation, which is defined as follows:

$$\sigma_{\text{SF}}(\theta) = -\sin^2 \theta, \quad (1a)$$

$$\sigma_{\text{SDF}}(\theta) = \cos^2 \theta, \quad (1b)$$

$$\sigma_{\text{SF-SDF}}(\theta) = \cos(2\theta). \quad (1c)$$

The solution domain is set as  $-\pi \leq \theta \leq +\pi$ . Note that, in all the cases the local nonlinearity coefficient (1) has its maxima at points  $\theta = 0$  and  $\theta = \pm\pi$ , and minima at  $\theta = \pm\pi/2$ . We aim to find basic types of modes trapped in rotating nonlinearity profiles (1), and establish their basic properties, such as symmetry/asymmetry, stability, and the identification of the respective ground states, varying two control parameters, *viz.*, the rotation speed,  $\omega$ , and the total power (norm),  $P$ , which is defined below in Eq. (20).

The paper is structured as follows. In Section II, we formulate the system and methods of the stability analysis of the modes. In Section III, we present numerical results for the basic modes and their stability in each type of the nonlinear potential (1). In Section IV, we present analytical results, obtained by means of a two-mode approximation, which explain a boundary between the symmetric and asymmetric modes in each case. The paper is concluded by Section V.

## II. THE MODEL

The dynamics of the optical wave (or the BEC wave function) in the rotating ring is governed by the normalized one-dimensional NLSE (GPE), subject to the periodic boundary conditions:

$$i\frac{\partial}{\partial z}\psi = \left[ -\frac{1}{2}\frac{\partial^2}{\partial\theta^2} + \sigma(\theta - \omega z)|\psi|^2 \right] \psi, \quad (2)$$

$\psi(\theta) \equiv \psi(\theta + 2\pi)$ , where  $z$  is the propagation distance in the case of the optical waveguide, and the radius of the ring is scaled to be 1. It is more convenient to rewrite Eq. (2) in the rotating reference frame, with  $\theta' \equiv \theta - \omega z$ :

$$i\frac{\partial}{\partial z}\psi = \left[ -\frac{1}{2}\frac{\partial^2}{\partial\theta'^2} + i\omega\frac{\partial}{\partial\theta'} + \sigma(\theta')|\psi|^2 \right] \psi, \quad (3)$$

while the solution domain is defined as above, i.e.,  $-\pi \leq \theta' \leq +\pi$ . For the BEC trapped in the rotating potential, the respective GPE differs by replacing  $z$  with time  $t$ . Equation (3) conserves the total power (norm) of the field and its Hamiltonian (energy),

$$P = \int_{-\pi}^{+\pi} |\psi(\theta')|^2 d\theta', \quad (4)$$

$$H = \frac{1}{2} \int_{-\pi}^{+\pi} \left[ \left| \frac{\partial\psi}{\partial\theta'} \right|^2 + i\omega \left( \psi^* \frac{\partial\psi}{\partial\theta'} - \psi \frac{\partial\psi^*}{\partial\theta'} \right) + \sigma(\theta')|\psi|^4 \right] d\theta', \quad (5)$$

with the asterisk standing for the complex conjugate. Stationary modes with real propagation constant  $-\mu$  (in terms of BEC,  $\mu$  is the chemical potential) are sought for as

$$\psi(\theta', z) = \exp(-i\mu z) \phi(\theta'), \quad (6)$$

with complex function  $\phi(\theta')$  obeying equation

$$\mu\phi = \left[ -\frac{1}{2}\frac{d^2}{d\theta'^2} + i\omega\frac{d}{d\theta'} + \sigma(\theta')|\phi|^2 \right] \phi. \quad (7)$$

The periodic boundary conditions,  $\sigma(\theta' + 2\pi) = \sigma(\theta')$  and  $\psi(\theta' + 2\pi) = \psi(\theta')$ , make Eq. (3) invariant with respect to the *boost transformation*, which allows one to change the rotation speed from  $\omega$  to  $\omega - N$  with arbitrary integer  $N$ :

$$\psi(\theta', z; \omega - N) = \psi(\theta', z; \omega) \exp \left[ -iN\theta' + i \left( \frac{1}{2}N^2 - N\omega \right) z \right], \quad (8)$$

hence the speed may be restricted to interval  $0 \leq \omega < 1$ . Furthermore, Eq. (3) admits an additional invariance, relating solutions with opposite signs of the speed:  $\psi(\theta', z; \omega) = \psi^*(\theta', -z; -\omega)$ . If combined with boost  $\omega \rightarrow \omega + 1$ , the latter transformation demonstrates that the solutions with

$$\omega = 1/2 \pm \delta, \quad (9)$$

where  $\delta < 1/2$ , are tantamount to each other. Thus, the rotation speed may be eventually restricted to the fundamental interval,

$$0 \leq \omega \leq 1/2, \quad (10)$$

which plays the role of the first *rotational Brillouin zone*, cf. Ref. [30].

The dynamical stability of the stationary solutions has been investigated via numerical computation of eigenvalues for small perturbations, and verified by direct simulations of the perturbed evolution. The perturbed solutions are introduced as usual,

$$\psi = e^{-i\mu z} [\phi(\theta') + \varepsilon u(\theta') e^{i\lambda z} + \varepsilon v^*(\theta') e^{-i\lambda^* z}], \quad (11)$$

where  $\varepsilon$  is an infinitesimal amplitude of the disturbance,  $u(\theta')$  and  $v(\theta')$  are the corresponding eigenmodes, and  $\lambda$  the eigenfrequency. The substitution of ansatz (11) into Eq. (3) and linearization leads to the linear eigenvalue problem,

$$\begin{pmatrix} \mu - \hat{h} - i\omega \frac{\partial}{\partial\theta'} & -\sigma\phi^2 \\ \sigma(\phi^*)^2 & -\mu + \hat{h} - i\omega \frac{\partial}{\partial\theta'} \end{pmatrix} \begin{pmatrix} u \\ v \end{pmatrix} = \lambda \begin{pmatrix} u \\ v \end{pmatrix}, \quad (12)$$

where  $\hat{h} = -(1/2)\partial^2/\partial(\theta')^2 + 2\sigma|\phi|^2$  is the single-particle Hamiltonian. The underlying solution  $\phi$  is stable if Eq. (12) generates solely real eigenvalues. Lastly, stationary equation (7) was solved using numerical code ‘‘PCSOM’’ borrowed from Ref. [38].

TABLE I: Different species of stationary modes, labeled by input waveforms which generate them as solutions of Eq. (7).

Inputs	Types of modes
$\cos \theta'$	Symmetric (even)
$\sin \theta'$	Antisymmetric (odd)
$\sin^2 \theta'$	Second-harmonic (2H)
$b + \cos \theta', 0 < b \leq 1$	Symmetry-breaking
$b + \sin \theta', 0 < b \leq 1$	2H-breaking

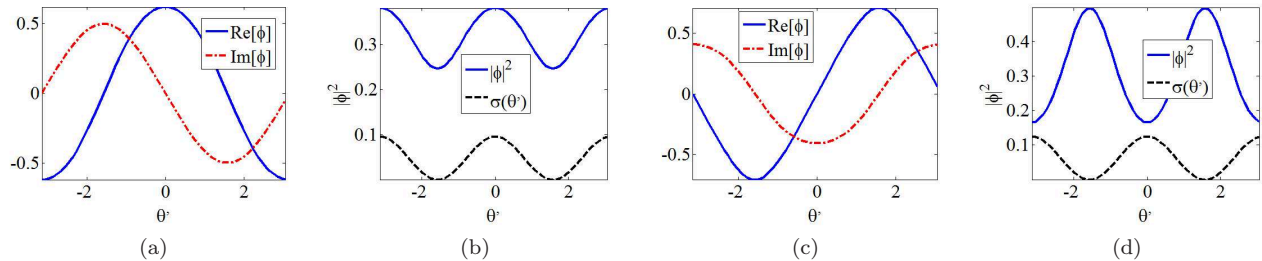


FIG. 2: (Color online) Examples of stable even and odd modes, found in the system with self-focusing nonlinear potential (1a), at rotation speed  $\omega = 0.25$ , with total power  $P_{\text{even}} = P_{\text{odd}} = 2$ . Panels (a), (c) display, severally, real and imaginary parts of the even and odd modes, while (b), (d) show their local-power (density) profiles. The dashed curves in (b) and (d), and in similar panels displayed below, depict the corresponding nonlinearity-modulation profile,  $\sigma(\theta')$ ; in the present case, it is  $\cos^2 \theta'$ .

### III. NUMERICAL RESULTS

#### A. The classification of trapped modes

For all types of the nonlinear potentials defined in Eq. (1), the numerical solution of stationary equation (7) with different inputs (initial guesses) makes it possible to identify five basic species of stationary states, which are listed in Table I.

Following the symmetry of the nonlinearity-modulation patterns in Eq. (1), the modes are identified as symmetric (alias even) and antisymmetric (alias odd), with respect to the central point,  $\theta' = 0$ . The mode of the “second-harmonic” (2H, also even) type refers to the dominant term in its Fourier decomposition. The names of the last two modes in Table I come from the types of their symmetry breaking. In particular, the named of 2H-breaking mode is come from its spontaneous symmetry breaking via the 2H mode, which will be demonstrated in the following. Note that all the inputs displayed in the table are real functions, while the numerically found solutions of Eq. (7) with  $\omega \neq 0$  are actually complex. Naturally, real parts of the solutions generated by the real inputs indicated in the table have the same parity (even/odd) as the inputs, while the imaginary parts feature the opposite parity (odd/even) (the input of the 2H-breaking type does not feature a certain parity). It is shown below too that maxima and minima of the local power (density) of the even mode defined in the table coincide with the maxima and minima of the local nonlinearity,  $\sigma(\theta')$ , while for the odd and 2H modes the relation is the opposite, with the peak powers sitting in potential wells [see Eq. (1)], hence the odd and 2H modes tend to have lower values of the energy, and may play the role of the ground state, as confirmed below.

#### B. The self-focusing nonlinearity

The SF nonlinear potential, defined as per Eq. (1a), gives rise to four types of dynamically stable trapped modes, *viz.*, even (symmetric), odd (antisymmetric), 2H and 2H-breaking ones (i.e., only the symmetry-breaking species is missing in this case). Typical examples of these stable modes are displayed in Figs. 2 and 3. In addition to the above-mentioned fact that the maxima and minima of the local power coincide with those of the nonlinear potential for the even mode, and, on the contrary, coincide with minima and maxima of the potential for the odd and 2H modes, suggesting that either of the latter modes may be a ground state, the figures demonstrate that the 2H-breaking mode has one maximum and one minimum of the local power, both sitting in nonlinear-potential wells (minima).

Results of the numerical analysis for the stability of the modes in the model with the SF nonlinear potential are

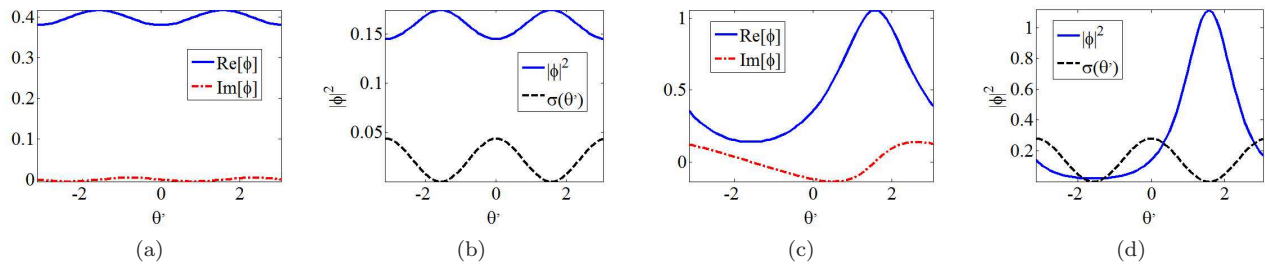


FIG. 3: (Color online) Examples of stable 2H and 2H-breaking modes, found in the system with the self-focusing nonlinear potential at  $\omega = 0.25$  and  $P_{2H} = 1$  and  $P_{2H\text{-break}} = 2$ , respectively. Panels have the same meaning as in Fig. 2.

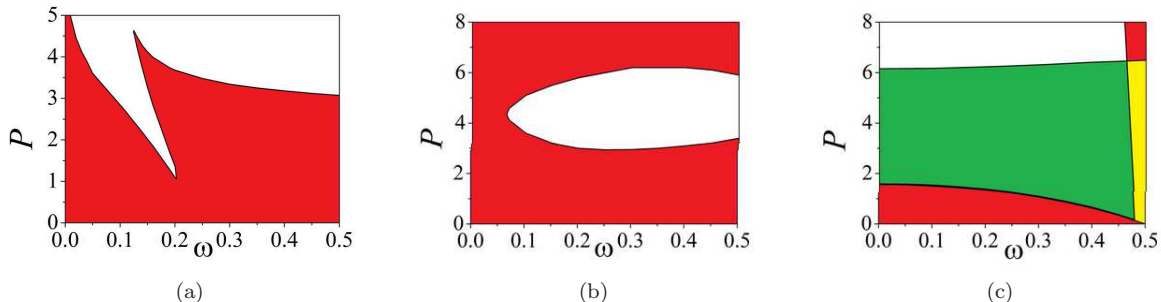


FIG. 4: (Color online) (a) and (b): Stability diagrams for the even and odd (antisymmetric) modes, respectively, obtained in the system with of the self-focusing nonlinearity, in the plane of the rotation speed ( $\omega$ ) and total power ( $P$ ). (c) The stability diagram for the set of the second-harmonic (2H) and 2H-breaking modes. In panels (a), (b), and (c), respectively, the even, odd, and 2H modes are stable in the red areas, and unstable in the blank ones. In panel (c), the 2H-breaking mode is stable in the green (middle) area, and the bistability, i.e., coexistence of 2H and 2H-breaking stable modes, occurs in the yellow (right edge) region. In the blank area of panel (c), no 2H-breaking mode, stable or unstable one, is found.

summarized in Fig. 4, in the form of diagrams drawn in the plane of  $(P, \omega)$ . They show that the stability regions of the even, odd, 2H and 2H-breaking modes strongly overlap between themselves. In particular, the asymmetry parameter of the 2H-breaking modes, which is defined as

$$\text{ASP} \equiv \left| \int_0^\pi |\phi|^2 d\theta' - \int_{-\pi}^0 |\phi|^2 d\theta' \right| / P, \quad (13)$$

is displayed in Figs. 5(a) and 5(b). The plots demonstrate that the transition between 2H and 2H-breaking modes is of the *supercritical* type [39].

The multistability, which is obvious in Fig. 4, makes it necessary to compare energies of the coexisting dynamically stable modes, defined by Eq. (5), in order to identify the ground state that realizes the energy minimum. First, in Fig. 6(a) we show the results along horizontal cuts of all the three panels of Fig. 4, made at a constant value of the total power,  $P = 0.5$ , with the rotation speed varying in the interval of  $0 \leq \omega \leq 0.4$ . The *tristability* of the even, odd and 2H modes takes place along this segment. Further, Fig. 6(b) displays the results along vertical cuts of panel (c) of Fig. 4 made at  $\omega = 0.5$ , while the power is varying as  $0.2 \leq P \leq 1.6$  [it is seen in panels (b) and (c) of Fig. 4 that the 2H-breaking mode also coexists with the stable odd one, but the energy of the odd mode is definitely larger, therefore it is not displayed in Fig. 6(b)]. In panel (b) of Fig. 6, the two branches merge into one, with  $H \rightarrow 0$ , at  $P \rightarrow 0$ , as the *nonlinear* potential vanishes in this limit.

From Fig. 6(a), we conclude that  $H_{2H} < H_{\text{odd}} < H_{\text{even}}$ , while Fig. 6(b) shows that  $H_{2H\text{-break}} < H_{2H}$ . Calculations of the energy, performed along other horizontal and vertical cuts, demonstrate that the following relation between the energies of the different modes, suggested by these inequalities, is always correct:

$$H_{2H\text{-break}} < H_{2H} < H_{\text{odd}} < H_{\text{even}}. \quad (14)$$

Thus, the 2H-breaking mode, if it exists [recall that, in the plane of  $(\omega, P)$  shown in Fig. 4(b), it exists above the curve separating the bottom (red) and middle (yellow) areas], represents the ground state in the system with the self-focusing nonlinearity. If the latter mode does not exist, then the 2H state plays the same role.

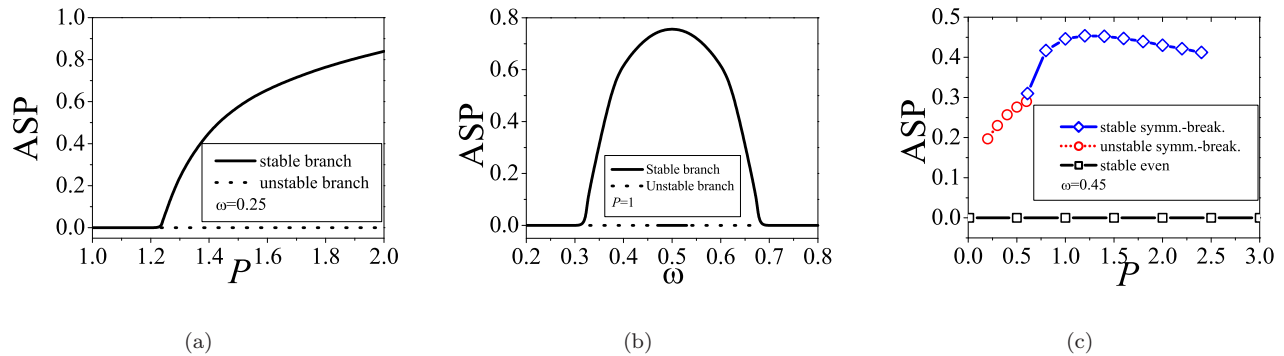


FIG. 5: (Color online) (a) The ASP of the 2H and 2H-breaking modes, defined as per Eq. (13), as a function of the total power,  $P$ , with the rotation speed fixed at  $\omega = 0.25$ , in the system with the self-focusing nonlinearity (b). The same as a function of  $\omega$ , at a fixed total power,  $P = 1$ . The plot includes regions symmetric with respect to  $\omega = 0.5$ , to stress the respective symmetry of modes in the present system. (c) The ASP of even and symmetry-breaking mode as a function of  $P$  for  $\omega = 0.45$ , in the case of the self-defocusing nonlinearity

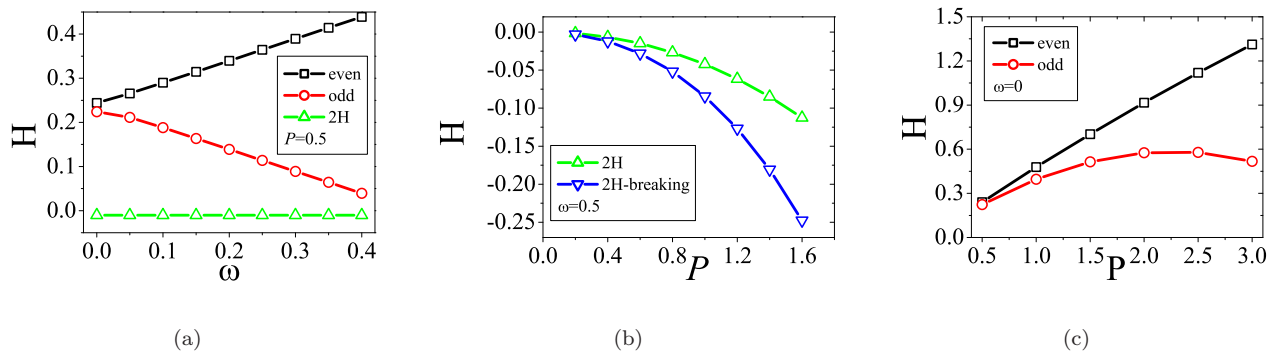


FIG. 6: (Color online) (a) Energies of the even, odd, and second-harmonic modes in the system with the self-focusing nonlinearity, computed, as per Eq. (5), for  $P = 0.5$  and  $0 \leq \omega \leq 0.4$ . (b) Energies of the 2H-breaking and second-harmonic modes, computed for  $\omega = 0.5$  and  $0.2 \leq P \leq 1.6$ . (c) Energies of the even and odd modes along the vertical segment, with  $\omega = 0$  and  $0.5 \leq P \leq 3$ .

In Fig. 6(a), we can see that in the limit of  $\omega = 0$ , the energies of the even and odd modes are very close, which seems in contradiction with the fact that these two modes are essentially different, having the opposite parities. The reason is that the total power that we chose here ( $P = 0.5$ ) is not large enough to show the energy difference between the two modes. To clarify the point, in Fig. 6(c) we display the energy curves for these two modes selected along the vertical segment with  $\omega = 0$  and  $0.5 \leq P \leq 3$ . It shows that the energy difference indeed increases with the growth of  $P$ .

### C. The self-defocusing nonlinearity

In the case of the SDF nonlinear potential, represented by Eq. (1b), the numerical solution of Eq. (7) reveals stable modes of three types, *viz.*, even, symmetry-breaking, and 2H (recall that symmetry-breaking modes were not found in the system with the SF nonlinearity), while odd and 2H-breaking states do not exist in this case. Because the profiles of the even and 2H modes are quite similar to their counterparts presented above in Fig. 2, we here display, in Fig. 7, only a typical stable symmetry-breaking mode. The shape of this mode seems symmetric, centered at  $\theta' = 0$ ; however, it is classified as an asymmetric mode, as the power profile of a true symmetric state would be double-humped, cf. Figs. 2(b,d) and 3(b), while the present one has a single maximum, similar to the intensity distribution in the 2H-breaking state in Fig. 3(d). Accordingly, the ASP (effective asymmetry measure) for the symmetry-breaking mode is



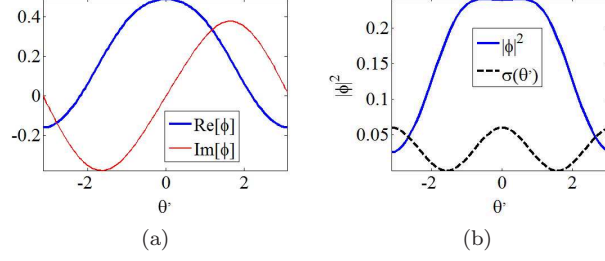


FIG. 7: (Color online) A stable symmetry-breaking mode, found in the system with the self-defocusing nonlinearity, at  $(\omega, P) = (0.45, 1)$ : (a) its real and imaginary parts; (b) the power profile.

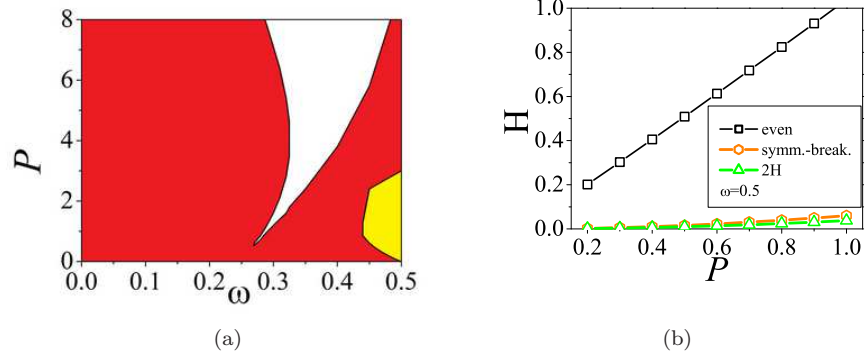


FIG. 8: (Color online) (a) The stability diagram for the even and symmetry-breaking modes in the system with the self-defocusing nonlinearity. The red (largest) and yellow (smallest, near the right edge) areas designate, severally, the stability region of the even mode, and the region of the coexistence (bistability) of the even and symmetry-breaking modes. In the blank area, no stable modes of these types are found (in fact, an unstable even mode exists in that area). The second-harmonic mode exists and is stable in the entire plane. (b) Energies of the even, symmetry-breaking, and second-harmonic modes along the vertical cut of panel (a) at  $\omega = 0.5$  and  $0.2 \leq P \leq 1$ .

introduced as follows, instead of the above definition (13):

$$(\text{ASP})_{\text{symm-break}} \equiv \left| \left[ \int_{-\pi/2}^{+\pi/2} - \left( \int_{-\pi}^{-\pi/2} + \int_{+\pi/2}^{+\pi} \right) \right] |\phi|^2 d\theta' \right| / P, \quad (15)$$

to stress the lack of the asymmetry between the central and peripheral parts of the mode.

The stability and energy diagrams for the even, symmetry-breaking, and 2H modes are displayed in Fig. 8 [the 2H mode exists and is stable in the entire plane of  $(P, \omega)$ , therefore it is not specially marked in panel 8(a)]. In particular, it is observed that the symmetry-breaking mode exists near the right edge of the rotational Brillouin zone, i.e., it does not exist in the stationary system (with  $\omega = 0$ ). The ASP of the even and symmetry-breaking modes, defined per Eq. (15), is displayed in Fig. 5(c) as a function of the total power. The absence of the linkage between the branches representing these two modes implies that they are not related by any bifurcation.

Figure 8(b) displays the comparison of energies of these three kinds of the modes (even, symmetry-breaking, and 2H ones) along the vertical cut made at  $\omega = 0.5$ , with the power varying in interval  $0.2 \leq P \leq 1$ . It demonstrates that the curve for the 2H mode goes close to but slightly lower than its counterpart for the symmetry-breaking mode. The analysis of more general data, produced by the numerical calculations for the system with the SDF nonlinear potential, demonstrates that energies of all the three dynamically stable modes existing in this case are ordered as follows:

$$H_{2\text{H}} < H_{\text{symm-break}} < H_{\text{even}}, \quad (16)$$

cf. Eq. (14). Thus, the 2H mode plays the role of the ground state in the case of the SDF nonlinearity (recall this mode exists at all values of  $\omega$  and  $P$ ).

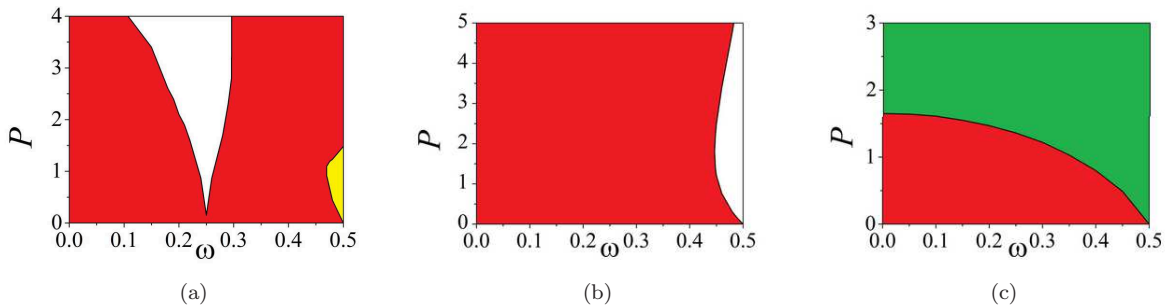


FIG. 9: (Color online) Stability diagrams for the system with the alternating self-focusing – self-defocusing nonlinearity. (a) Even and symmetry-breaking modes; (b) odd and 2H-breaking modes; (c) the 2H modes. In (a), the even mode is stable in the red (bottom) area; in the small yellow region it coexists with the symmetry-breaking one, and no stable modes of these types are found in the blank area. In (b), the odd mode is stable in the red (bottom) area, the 2H-breaking mode is stable in the green region (adjacent to the right edge of the panel), and these two types coexist in the yellow area. In (c), the 2H mode is stable in the red area.

#### D. The alternating self-focusing – self-defocusing nonlinear potential

In the case of the alternating SF-SDF nonlinearity, defined as per Eq. (1), the numerical solutions reveal the existence of all the five types of stable trapped modes indicated in Table I. Profiles of these modes are quite similar to those of their counterparts displayed above in Figs. 2, 3, and 7, therefore we do not show them again here. The respective stability diagrams in the  $(P, \omega)$  plane are presented in Fig. 9. In particular, the absence of a bistability area in panel (c) of Fig. 9 suggests that the transition between the 2H and 2H-breaking modes is supercritical, like in the system with the SF nonlinearity, cf. Fig. ??.

The comparison of the energies of the five types of the modes which may be stable in the case of the sign-alternating nonlinearity demonstrates the following ordering, cf. Eqs. (14) and (16):

$$H_{2H\text{-break}} < H_{2H} < H_{\text{symm.-break}}, H_{\text{odd}} < H_{\text{even}}. \quad (17)$$

The energies of the symmetry-breaking and odd modes are not compared in Eq. (17), as their stability regions do not overlap, see Fig. 9(a,b). Thus, the 2H-breaking mode, when it exists, plays the role of the ground state in the present case; otherwise, the ground state is represented by the 2H mode, see panels (b) and (c) in Fig. 9.

### IV. THE ANALYTICAL APPROACH

#### A. The two-mode approximation

The present setting may be naturally approximated by a finite-mode truncation of the expansion of stationary field  $\phi(x)$  over the set of spatial harmonics. The simplest approximation reduces to the substitution of truncation

$$\phi(\theta') = a_0 + a_1 \exp(i\theta') \quad (18)$$

into Eq. (7). In this expression,  $a_0$  may be fixed to be real, while amplitude  $a_1$  is allowed to be complex. This approach is consistent if, in the linear approximation, each term in combination (18) is an exact solution of Eq. (7) for a common value of  $\mu$ , hence the zeroth-order approximation exists, and the analysis of weakly nonlinear states can be developed around it. It is easy to see that such a case corresponds, in the zeroth approximation, to  $\omega = 1/2$  [which is exactly the right edge of zone (10)] and  $\mu = 0$  [34]. Then, weakly nonlinear modes can be constructed in an approximate analytical form, assuming that  $\mu$ ,  $a_0^2$ ,  $|a_1|^2$ , and

$$\delta \equiv 1/2 - \omega \quad (19)$$

are all small quantities. To this end, ansatz (18) and a particular expression (1) for  $\sigma(\theta')$  are substituted into Eq. (7), and equations for amplitudes  $a_0$  and  $a_1$  are derived as balance conditions for the zeroth and first harmonics.

Ansatz (18) corresponds to the following approximation for the total power (4),

$$P = \int_{-\pi}^{+\pi} |\phi|^2 d\theta' = 2\pi(a_0^2 + |a_1|^2), \quad (20)$$



which will be used below too.

### B. The self-focusing nonlinearity

In the case of the SF nonlinear potential (1a), the two-mode approximation (18) leads to the following equations:

$$\begin{aligned}\mu &= -\frac{1}{2}a_0^2 - |a_1|^2 + \frac{1}{4}a_1^2, \\ \mu - \delta &= -a_0^2 - \frac{1}{2}|a_1|^2 + \frac{1}{4}a_0^2 \frac{a_1^*}{a_1}.\end{aligned}\quad (21)$$

As shown above by the numerical analysis, the SF nonlinearity gives rise, *inter alia*, to the 2H-breaking mode, which is generated from input  $b + \sin \theta'$  in Table I. To capture the part of the solution corresponding to  $\sin \theta'$  in the input, we set

$$a_1 = ic, \quad (22)$$

Then, Eq. (21) yields

$$\begin{aligned}a_0^2 &= (4/21)(5\delta - 3\mu), \\ c^2 &= -(4/21)(2\delta + 3\mu).\end{aligned}\quad (23)$$

Substituting solution (23) into expression (20), we obtain a relation between the propagation constant and total power for the 2H-breaking mode,

$$\mu = \frac{\delta}{2} - \frac{7}{16\pi}P. \quad (24)$$

It demonstrates that this mode, as predicted by the analytical approximation, satisfied the Vakhitov-Kolokolov (VK) criterion,  $d\mu/dP < 0$ , which is a necessary stability condition for patterns supported by the SF nonlinearity [40].

Furthermore, Eq. (23) predicts the emergence of the 2H-breaking modes at  $a_0^2 = 0$ , i.e.,

$$\mu = 5\delta/3. \quad (25)$$

Since the modes with rotation speeds related by Eq. (9) are mutually tantamount, Eqs. (25) and (24) predict the coexistence of the odd and 2H-breaking modes at

$$P \geq (P_{\min}) = (8\pi/3)|\delta|. \quad (26)$$

This analytical result is compared with the corresponding numerical findings in Fig. 10(a), which shows a reasonably good agreement.

### C. The self-defocusing nonlinearity

The substitution of the same ansatz (18) into Eq. (7) in the case of the SDF nonlinear potential, taken as per Eq. (1b), yields the following algebraic equations, instead of Eq. (21) derived above for the SF nonlinearity:

$$\begin{aligned}\mu &= \frac{1}{2}a_0^2 + |a_1|^2 + \frac{1}{4}a_1^2, \\ \mu - \delta &= a_0^2 + \frac{1}{2}|a_1|^2 + \frac{1}{4}a_0^2 \frac{a_1^*}{a_1}.\end{aligned}\quad (27)$$

The above numerical results for the SDF nonlinearity demonstrate the existence of the symmetry-breaking mode in this case, which is generated by input  $b + \cos \theta'$  in Table I. To capture this mode by means of ansatz (18), it is natural to set

$$a_1 = c \equiv \text{real}, \quad (28)$$

on the contrary to Eq. (22), where  $a_1$  was imaginary. In this case, the algebraic system (27) yields

$$\begin{aligned} a_0^2 &= (4/21) (3\mu - 5\delta), \\ c^2 &= (4/21) (3\mu + 2\delta), \end{aligned} \quad (29)$$

cf. Eq. (23). According to Eq. (20), the relations between the propagation constant and total power takes the following form for solution (29):

$$\mu = \frac{\delta}{2} + \frac{7}{16\pi}P, \quad (30)$$

cf. Eq. (24). This equation demonstrates that the asymmetric mode satisfies the *anti-VK* criterion,  $d\mu/dP > 0$ , which, as argued in Ref. [41], may play the role of a necessary stability condition for modes supported by the SDF nonlinearity.

The analytical approximation predicts the existence boundary for the symmetry-breaking states,  $a_0^2 = 0$ , in the same form (25) as it was obtained above for the SF nonlinearity. Consequently, the existence region for these states is predicted in the form coinciding with that given by Eq. (26). This result is compared with its numerical counterpart in Fig. 10(b).

#### D. The alternating self-focusing – self-defocusing nonlinearity

In the case of the alternating SF-SDF nonlinear potential (1c), the substitution of ansatz (18) into Eq. (7) yields the algebraic equations in the form which is somewhat simpler than Eqs. (21) and (27) derived above for the “pure” SF and SDF nonlinearities:

$$\begin{aligned} \mu &= \frac{1}{2}a_1^2, \\ \mu - \delta &= \frac{1}{2}a_0^2 \frac{a_1^*}{a_1}. \end{aligned} \quad (31)$$

First, if we choose real  $a_1$ , as in Eq. (28), which refers to the symmetry-breaking mode, Eq. (31) yields

$$\begin{aligned} a_0^2 &= 2(\mu - \delta), \\ c^2 &= 2\mu. \end{aligned} \quad (32)$$

The corresponding relation between  $\mu$  and  $P$  is

$$\mu = \frac{\delta}{2} + \frac{P}{8\pi}, \quad (33)$$

which satisfies the above-mentioned anti-VK criterion, cf. Eq. (30), i.e., it is possible to assume that the stability of the symmetry-breaking mode is supported by the SDF part of the alternating nonlinear potential. Further, Eq. (32) predicts the emergence of the symmetry-breaking mode ( $a_0^2 = 0$ ) at  $\mu = \delta$ . In terms of the total power related to  $\mu$  by Eq. (20), this implies that this mode exists at

$$P \geq P_{\min} = 4\pi|\delta|, \quad (34)$$

cf. Eq. (26). The comparison of this analytical result with its numerical counterpart is shown in Fig. 10(c).

The numerical results presented in the previous section demonstrate that the alternating SF-SDF nonlinear potential support the stable 2H-breaking mode too. To describe it in the framework of the two-mode approximation, we now assume  $a_1$  to be imaginary, as in Eq. (22). In this case, Eq. (32) yields

$$\begin{aligned} a_0^2 &= 2(\delta - \mu), \\ c^2 &= -2\mu, \end{aligned} \quad (35)$$

cf. Eq. (31), the respective relation between  $\mu$  and  $P$  being

$$\mu = \frac{\delta}{2} - \frac{P}{8\pi}, \quad (36)$$

cf. Eq. (33). The latter relation satisfies the VK criterion, which implies that the stability of the 2H-breaking mode is supported by the SF part of the alternating nonlinear potential. The emergence of the 2H-breaking mode corresponds to  $a_0^2 = 0$ , i.e., again  $\mu = \delta$ , as in the case of the symmetry-breaking mode, under the same alternating nonlinear potential. Finally, this means that the existence of the stable 2H-breaking mode is predicted in the same region (34) as for its symmetry-breaking counterpart. The latter prediction is compared to the numerical findings in Fig. 10(d).

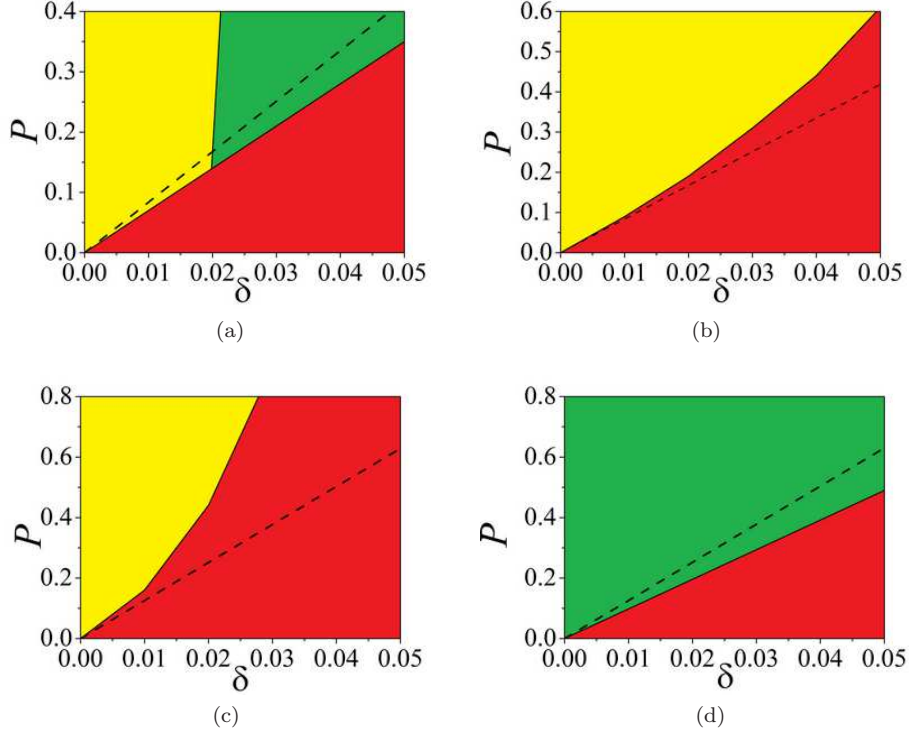


FIG. 10: (Color online) The comparison between the theoretically predicted (dashed lines) and numerically found boundaries of the existence of the stable 2H-breaking (a,d) and symmetry-breaking (b,c) modes in the plane of  $(\delta, P)$ , in the interval of  $0 \leq |\delta| \equiv |1/2 - \omega| \leq 0.05$ . In the red areas, only even or 2H modes are produced by the numerical solution, while in the yellow (bistability) regions they coexist with the stable symmetry- or 2H-breaking modes, respectively. Panels (a) and (b) pertain, severally, to the SF and SDF nonlinear potentials, while (c) and (d) correspond to the alternating SF-SDF potential. These four panels are, actually, zoomed versions of the right bottom corners of Figs. 4(b), 8(a), 9(a), and 9(b), respectively, with analytically predicted lines (26) or (34) added to each panel.

## V. CONCLUSION

This work aimed to study the existence and stability of modes trapped in the rotating nonlinear-lattice potentials of the SF, SDF (self-focusing and defocusing) and alternating SF-SDF types. The consideration was carried out for the first rotational Brillouin zone in the rotating reference frame, i.e., for  $0 \leq \omega \leq 1/2$ , where  $\omega$  is the rotation speed. The stability analysis was performed through the computation of eigenvalues for small perturbations, and verified by direct simulations. The model can be realized in the spatial domain, in terms of a twisted-pipe optical waveguide, with the built-in azimuthal modulation of the local Kerr coefficient, or, in the temporal domain, as the Gross-Pitaevskii equation for BEC loaded into a toroidal trap, under the action of a rotating optical or magnetic structure which affects the local value of the scattering length.

In the SF system, four types of different modes have been identified: even, odd, which are dominated by combinations of the fundamental and zeroth angular harmonic, and the 2H (second-harmonic) and 2H-breaking states. On the other hand, the SDF nonlinear potential supports three species of the trapped states: 2H, even, and symmetry-breaking ones, the latter existing only at the rotation speed close to the right edge of the Brillouin zone,  $\omega = 1/2$ , and in a limited interval of values of the total power,  $P$ . As for the alternating SF-SDF nonlinear potential, it supports all the five species of the trapped modes. Transitions between the 2H and 2H-breaking modes are of the supercritical types. The energy comparison reveals that, in the SF and SF-SDF systems alike, the 2H-breaking mode, if it exists, represents the ground state; otherwise, this role is played by the 2H mode. The ground state of the SDF system is always represented by the 2H solution.

This work may be naturally developed in other directions. On the one hand, it is relevant to consider rotating nonlinear lattices with smaller azimuthal periods,  $2\pi/n$ , for integer  $n > 1$ , unlike the case of  $n = 1$  investigated here. On the other hand, it may be interesting to consider a two-dimensional version of the present one-dimensional model (with an entire rotating plane, rather than the thin ring, which will include effects of the Coriolis' force).

## Acknowledgments

We appreciate a valuable discussion with Dimitri J. Frantzeskakis, and help in the use of numerical methods provided by Nir Dror and Shenhe Fu. This work was supported by CNNSF (grant No. 11104083, 11204089, 11205063), by the German-Israel Foundation through grant No. I-1024-2.7/2009, and by the Tel Aviv University in the framework of the “matching” scheme.

- 
- [1] Y. V. Kartashov, B. A. Malomed, and L. Torner, *Rev. Mod. Phys.* **83**, 247 (2011).
- [2] W. A. Harrison, *Pseudopotentials in the Theory of Metals* (Benjamin: New York, 1966).
- [3] F. K. Abdullaev, A. Gammal, and L. Tomio, *J. Phys. B* **37**, 635 (2004); H. Sakaguchi and B. A. Malomed, *Phys. Rev. E* **72**, 046610 (2005); F. K. Abdullaev and J. Garnier, *Phys. Rev. A* **72**, 061605(R) (2005); G. Theocharis, P. Schmelcher, P. G. Kevrekidis, and D. J. Frantzeskakis, *ibid.* **72**, 033614 (2005); D. L. Machacek, E. A. Foreman, Q. E. Hoq, P. G. Kevrekidis, A. Saxena, D. J. Frantzeskakis, and A. R. Bishop, *Phys. Rev. E* **74**, 036602 (2006); P. Niarchou, G. Theocharis, P. G. Kevrekidis, P. Schmelcher, and D. J. Frantzeskakis, *Phys. Rev. A* **76**, 023615 (2007); Z. Rapti, P. G. Kevrekidis, V. V. Konotop, and C. K. R. T. Jones, *J. Phys. A* **40**, 14151 (2007); F. Abdullaev, A. Abdumalikov, and R. Galimzyanov, *Phys. Lett. A* **367**, 149 (2007); F. K. Abdullaev, A. Gammal, M. Salerno, and L. Tomio, *Phys. Rev. A* **77**, 023615 (2008); L. C. Qian, M. L. Wall, S. Zhang, Z. Zhou, and H. Pu, *ibid.* **77**, 013611 (2008); A. S. Rodrigues, P. G. Kevrekidis, M. A. Porter, D. J. Frantzeskakis, P. Schmelcher, and A. R. Bishop, *ibid.* **78**, 013611 (2008); F. K. Abdullaev, Y. V. Bludov, S. V. Dmitriev, P. G. Kevrekidis, and V. V. Konotop, *Phys. Rev. E* **77**, 016604 (2008); Y. V. Kartashov, B. A. Malomed, V. A. Vysloukh, and L. Torner, *Opt. Lett.* **34**, 3625 (2009); F. K. Abdullaev, R. M. Galimzyanov, M. Brtko, and L. Tomio, *Phys. Rev. E* **79**, 056220 (2009); N. Dror and B. A. Malomed, *Phys. Rev. A* **83**, 033828 (2011); X.-F. Zhou, S.-L. Zhang, Z.-W. Zhou, B. A. Malomed, and H. Pu, *ibid.* **85**, 023603 (2012).
- [4] H. Sakaguchi and B. A. Malomed, *Phys. Rev. E* **73**, 026601 (2006); G. Fibich, Y. Sivan, and M. I. Weinstein, *Physica D* **217**, 31 (2006); Y. Sivan, G. Fibich, and M. I. Weinstein, *Phys. Rev. Lett.* **97**, 193902 (2006); Y. V. Kartashov, B. A. Malomed, V. A. Vysloukh, and L. Torner *Opt. Lett.* **34**, 770 (2009); *Phys. Rev. A* **80**, 053816 (2009); O. V. Borovkova, B. A. Malomed, Y. V. Kartashov, *EPL* **92**, 64001 (2010); N. V. Hung, P. Ziří, M. Trippenbach, and B. A. Malomed, *Phys. Rev. E* **82**, 046602 (2010); T. Mayteevarunyoo, B. A. Malomed, and A. Reksabutr, *J. Mod. Opt.* **58**, 1977 (2011); H. Sakaguchi and B. A. Malomed, *Opt. Lett.* **37**, 1035 (2012).
- [5] T. Mayteevarunyoo, B. A. Malomed, and G. Dong, *Phys. Rev. A* **78**, 053601 (2008); O. V. Borovkova, V. E. Lobanov, and B. A. Malomed, *ibid.* **85**, 023845 (2012); A. Acus, B. A. Malomed, and Y. Shnir, *Physica D* **241**, 987 (2012).
- [6] O. V. Borovkova, Y. V. Kartashov, B. A. Malomed, and L. Torner, *Opt. Lett.* **36**, 3088 (2011); O. V. Borovkova, Y. V. Kartashov, L. Torner, and B. A. Malomed, *Phys. Rev. E* **84**, 035602 (R) (2011); W.-P. Zhong, M. Belić, G. Assanto, B. A. Malomed, and T. Huang, *Phys. Rev. A* **84**, 043801 (2011); Y. V. Kartashov, V. A. Vysloukh, L. Torner, and B. A. Malomed, *Opt. Lett.* **36**, 4587 (2011); V. E. Lobanov, O. V. Borovkova, Y. V. Kartashov, B. A. Malomed, and L. Torner, *ibid.* **37**, 1799 (2012).
- [7] F. Luan, A. K. George, T. D. Hedley, G. J. Pearce, D. M. Bird, J. C. Knight, and P. St. J. Russell, *Opt. Lett.* **29**, 2369 (2004); G. Bouwmans, L. Bigot, Y. Quiquempois, F. Lopez, L. Provino, and M. Douay, *Opt. Exp.* **13**, 8452 (2005); A. Fuerbach, P. Steinvurzel, J. A. Bolger, A. Nulsen, and B. J. Eggleton, *Opt. Lett.* **30**, 830 (2005).
- [8] T. T. Larsen, A. Bjarklev, D. S. Hermann, and J. Broeng, *Opt. Exp.* **11**, 2589 (2003); F. Du, Y. Q. Lu, and S. T. Wu, *Appl. Phys. Lett.* **85**, 2181 (2004); M. W. Haakestad, T. T. Alkeskjold, M. D. Nielsen, L. Scolari, J. Riishede, H. E. Engan, and A. Bjarklev, *IEEE Phot. Tech. Lett.* **17**, 819 (2005); C. R. Rosberg, F. H. Bennet, D. N. Neshev, P. D. Rasmussen, O. Bang, W. Królikowski, A. Bjarklev, and Y. S. Kivshar, *Opt. Exp.* **15**, 12145 (2007).
- [9] J. Hukriede, D. Runde, and D. Kip, *J. Phys. D* **36**, R1 (2003).
- [10] J. Li, B. Liang, Y. Liu, P. Zhang, J. Zhou, S. O. Klimonsky, A. S. Slesarev, Y. D. Tretyakov, L. O. Faolain, and T. F. Krauss, *Adv. Mater.* **22**, 1 (2010); M. Feng, Y. Liu, Y. Li, X. Xie, and J. Zhou, *Opt. Exp.* **19**, 7222 (2011); Y. Li, B. A. Malomed, J. Wu, W. Pang, S. Wang, and J. Zhou, *Phys. Rev. A* **84**, 043839 (2011); B. Liang, Y. Liu, J. Li, L. Song, Y. Li, J. Zhou and K. S. Wong, *J. Micromech. Microeng.* **22** 035013 (2012).
- [11] Y. Li, B. A. Malomed, M. Feng, and J. Zhou, *Phys. Rev. A* **82** 063813 (2010); W. Pang, J. Wu, Z. Yuan, Y. Liu and G. Chen, *J. Phys. Soc. Jpn.* **80**, 113401 (2011); J. Wu, M. Feng, W. Pang, S. Fu, and Y. Li, *J. Nonlin. Opt. Phys.* **20**, 193 (2011); Y. Li, W. Pang, S. Fu, and B. A. Malomed, *Phys. Rev. A* **85**, 053821 (2012).
- [12] M. Fleischhauer, A. Imamoğlu, and J. P. Marangos, *Rev. Mod. Phys.* **77**, 633 (2005); H. Schmidt and A. Imamoğlu, *Opt. Lett.* **21**, 1936 (1996); H. Wang, D. Goorskey, and M. Xiao, *Phys. Rev. Lett.* **87**, 073601 (2001).
- [13] S. Inouye, M. R. Andrews, J. Stenger, H. J. Miesner, D. M. Stamper-Kurn, and W. Ketterle, *Nature (London)* **392**, 151 (1998); Ph. Courteille, R. S. Freeland, D. J. Heinzen, F. A. van Abeelen, and B. J. Verhaar, *Phys. Rev. Lett.* **81**, 69 (1998); J. L. Roberts, N. R. Claussen, J. P. Burke, C. H. Greene, E. A. Cornell, and C. E. Wieman, *ibid.* **81**, 5109 (1998).
- [14] P. O. Fedichev, Y. Kagan, G. V. Shlyapnikov, and J. T. M. Walraven, *Phys. Rev. Lett.* **77**, 2913 (1996); M. Theis, G. Thalhammer, K. Winkler, M. Hellwig, G. Ruff, R. Grimm, and J. H. Denschlag, *ibid.* **93**, 123001 (2004).
- [15] S. Ghanbari, S., T. D. Kieu, A. Sidorov, and P. Hannaford, *J. Phys. B* **39**, 847 (2006); A. Abdelrahman, P. Hannaford, and K. Alameh, *Opt. Express* **17**, 24358 (2009).
- [16] A. E. Fetter, *Rev. Mod. Phys.* **81**, 647 (2009).

- [17] P. Engels, I. Coddington, P. C. Haljan, V. Schweikhard, and E. A. Cornell, Phys. Rev. Lett. **90**, 170405 (2003).
- [18] A. L. Fetter, Phys. Rev. A **64**, 063608 (2001); E. Lundh, *ibid.* **65**, 043604 (2002); K. Kasamatsu, M. Tsubota, and M. Ueda, *ibid.* **66**, 053606 (2002); G. M. Kavoulakis and G. Baym, New J. Phys. **5**, 51 (2003); A. Aftalion and I. Danaila, Phys. Rev. A **69**, 033608 (2004); U. R. Fischer and G. Baym, Phys. Rev. Lett. **90**, 140402 (2003); A. D. Jackson and G. M. Kavoulakis, Phys. Rev. A **70**, 023601 (2004); T. K. Ghosh, *ibid.* **69**, 043606 (2004).
- [19] K. Kasamatsu and M. Tsubota, Phys. Rev. A **76**, 023606 (2009).
- [20] N. K. Wilkin, J. M. F. Gunn, and R. A. Smith, Phys. Rev. Lett. **80**, 2265 (1998); B. Mottelson, *ibid.* **83**, 2695 (1999); C. J. Pethick and L. P. Pitaevskii, Phys. Rev. A **62**, 033609 (2000); E. Lundh, A. Collin, and K.-A. Suominen, Phys. Rev. Lett. **92**, 070401 (2004); G. M. Kavoulakis, A. D. Jackson, and G. Baym, Phys. Rev. A **70**, 043603 (2004); A. Collin, *ibid.* **73**, 013611 (2006); A. Collin, E. Lundh, and K.-A. Suominen, Phys. Rev. A **71**, 023613 (2005); S. Bargi, G. M. Kavoulakis, and S. M. Reimann, *ibid.* **73**, 033613 (2006); H. Sakaguchi and B. A. Malomed, *ibid.* **78**, 063606 (2008).
- [21] V. Schweikhard, I. Coddington, P. Engels, S. Tung, and E. A. Cornell, Phys. Rev. Lett. **93**, 210403 (2004); S. Tung, V. Schweikhard, and E. A. Cornell, *ibid.* **97**, 240402 (2006).
- [22] J. W. Reijnders and R. A. Duine, Phys. Rev. Lett. **93**, 060401 (2004); Phys. Rev. A **71**, 063607 (2005); H. Pu, L. O. Baksmaty, S. Yi, and N. P. Bigelow, Phys. Rev. Lett. **94**, 190401 (2005); H. Pu, L. O. Baksmaty, S. Yi, and N. P. Bigelow, *ibid.* **94**, 190401 (2005); R. Bhat, L. D. Carr, and M. J. Holland, *ibid.* **96**, 060405 (2006); K. Kasamatsu and M. Tsubota, *ibid.* **97**, 240404 (2006); M. P. Mink, C. Morais Smith, and R. A. Duine, Phys. Rev. A **79**, 013605 (2009).
- [23] H. Sakaguchi and B. A. Malomed, Phys. Rev. A **75**, 013609 (2007); **79**, 043606 (2009).
- [24] R. A. Williams, S. Al-Assam, and C. J. Foot, Phys. Rev. Lett. **104**, 050404 (2010).
- [25] G. Kakarantzas, A. Ortigosa-Blanch, T. A. Birks, P. St. J. Russell, L. Farr, F. Couny, and B. J. Mangan, Opt. Lett. **28**, 158 (2003).
- [26] G. K. L. Wong, M. S. Kang, H. W. Lee, F. Biancalana, C. Conti, T. Weiss, and P. St. J. Russell, Science **337**, 446 (2012).
- [27] R. Y. Chiao and Y. S. Wu, Phys. Rev. Lett. **57**, 933 (1986); A. Tomita and R. Y. Chiao, *ibid.* **57**, 937 (1986); V. I. Kopp and A. Z. Genack, Opt. Lett. **28**, 1876 (2003); M. Ornigotti, G. Della Valle, D. Gatti, and S. Longhi, Phys. Rev. A **76**, 023833 (2007).
- [28] S. Jia and J. W. Fleischer, Phys. Rev. A **79**, 041804(R) (2009).
- [29] B. A. Malomed, Phys. Rev. A **43**, 410 (1991).
- [30] H. Saito and M. Ueda, Phys. Rev. Lett. **93**, 220402 (2004); S. Schwartz, M. Cozzini, C. Menotti, I. Carusotto, P. Bouyer, and S. Stringari, New J. Phys. **8**, 162 (2006).
- [31] Y. V. Kartashov, B. A. Malomed, and L. Torner, Phys. Rev. A **75**, 061602(R) (2007).
- [32] L. Wen, H. Xiong, and B. Wu, Phys. Rev. A **82**, 053627 (2010).
- [33] G. J. Milburn, J. Corney, E. M. Wright, and D. F. Walls, Phys. Rev. A **55**, 4318 (1997); I. Zapata, F. Sols, and A. J. Leggett, *ibid.* **57**, R28 (1998); E. A. Ostrovskaya, Y. S. Kivshar, M. Lisak, B. Hall, F. Cattani, and D. Anderson, *ibid.* **61**, 031601(2000); R. D'Agosta, B. A. Malomed, C. Presilla, Phys. Lett. A **275**, 424 (2000); R. K. Jackson and M. I. Weinstein, J. Stat. Phys. **116**, 881 (2004); K. W. Mahmud, H. Perry, and W. P. Reinhardt, Phys. Rev. A **71**, 023615 (2005); H. T. Ng and P. T. Leung, *ibid.* **71**, 013601 (2005); T. Schumm, S. Hofferberth, L. M. Andersson, S. Wildermuth, S. Groth, I. Bar-Joseph, J. Schmiedmayer and P. Krüger, Nature Physics **1**, 57 (2005); M. Albiez, R. Gati, J. Fölling, S. Hunsmann, M. Cristiani, and M. K. Oberthaler, Phys. Rev. Lett. **95**, 010402 (2005).
- [34] Y. Li, W. Pang, and B. A. Malomed, Phys. Rev. A **86** 023832 (2012).
- [35] S. Gupta, K. W. Murch, K. L. Moore, T. P. Purdy, and D. M. Stamper-Kurn, Phys. Rev. Lett. **95**, 143201 (2005); A. S. Arnold, C. S. Garvie, and E. Riis, Phys. Rev. A **73**, 041606(R) (2006); I. Lesanovsky and W. von Klitzing, *ibid.* **99**, 083001 (2007); C. Ryu, M. F. Andersen, P. Cladé, V. Natarajan, K. Helmerson, and W. D. Phillips, Phys. Rev. Lett. **99**, 260401 (2007); A. Ramanathan, K. C. Wright, S. R. Muniz, M. Zelan, W. T. Hill III, C. J. Lobb, K. Helmerson, W. D. Phillips, and G. K. Campbell, *ibid.* **106**, 130401 (2011).
- [36] L. Salasnich, A. Parola, and L. Reatto, Phys. Rev. A **74**, 031603(R) (2006); R. Kanamoto, H. Saito, and M. Ueda, *ibid.* **73**, 033611 (2006); M. Modugno, C. Tozzo, and F. Dalfovo, *ibid.* **74**, 061601 (R) (2006); A. V. Carpentier and H. Michinel, EPL **78**, 10002 (2007); P. Mason and N. G. Berloff, Phys. Rev. A **79**, 043620 (2009); J. Brand, T. J. Haigh, and U. Zülicke, *ibid.* **80**, 011602 (R) (2009); P. Capuzzi and D. M. Jezek, J. Phys. B: At. Mol. Opt. Phys. **42**, 145301 (2009); A. Aftalion and P. Maso, *ibid.* **81**, 023607 (2010); J. Smyrnakis, M. Magiropoulos, G. M. Kavoulakis, and A. D. Jackson, *ibid.* **81**, 063601 (2010); S. Zöllner, G. M. Bruun, C. J. Pethick, and S. M. Reimann, Phys. Rev. Lett. **107**, 035301 (2011); Z.-W. Zhou, S.-L. Zhang, X.-F. Zhou, G.-C. Guo, X. Zhou, and H. Pu, Phys. Rev. A **83**, 043626 (2011); M. Abad, M. Guilleumas, R. Mayol, M. Pi, and D. M. Jezek, *ibid.* **84**, 035601 (2011); X. Zhou, S. Zhang, Z. Zhou, B. A. Malomed, and H. Pu, *ibid.* **85**, 023603 (2012); S. K. Adhikari, *ibid.* **85**, 053631 (2012).
- [37] S. Schwartz, M. Cozzini, C. Menotti, I. Carusotto, P. Bouyer, and S. Stringari, New J. Phys. **8**, 162 (2006); J. Smyrnakis, S. Bargi, G. M. Kavoulakis, M. Magiropoulos, K. Kärkkäinen, and S. M. Reimann, Phys. Rev. Lett. **103**, 100404 (2009).
- [38] J. Yang and T. I. Lakoba, Stud. Appl. Math. **118**, 153 (2007); **120**, 265 (2008).
- [39] G. Iooss and D. D. Joseph, *Elementary Stability and Bifurcation Theory* (Springer, New York: 1980).
- [40] M. Vakhitov and A. Kolokolov, Izvestiya VUZov Radiofizika **16**, 1020 (1973) [in Russian; English translation: Radiophys. Quantum. Electron. **16**, 783 (1973)]; L. Bergé, Phys. Rep. **303**, 259 (1998); E. A. Kuznetsov and F. Dias, *ibid.* **507**, 43 (2011).
- [41] H. Sakaguchi and B. A. Malomed, Phys. Rev. A **81**, 013624 (2010).